Eur. J. Mineral.
2006, **18**, 105–112

Clinohydroxylapatite: a new apatite-group mineral from northwestern Ontario (Canada), and new data on the extent of Na-S substitution in natural apatites

ANTON R. CHAKHMOURADIAN[1]* and LUCA MEDICI[2]

[1]Department of Geological Sciences, University of Manitoba, Winnipeg, Manitoba, R3T 2N2, Canada
*Corresponding author, e-mail: chakhmou@ms.umanitoba.ca
[2]Istituto di Metodologie per l'Analisi Ambientale, Tito Scalo, 85050 Potenza, Italy

Abstract: A monoclinic analogue of the mineral hydroxylapatite was found in altered leucogabbro making up one of the intrusive units in the Mesoproterozoic Seagull pluton in northwestern Ontario, Canada. The mineral is part of a replacement assemblage developed metasomatically after igneous plagioclase. It occurs as masses of coalescent spherulites < 30 μm in diameter, and is paragenetically associated with prehnite, hibschite, titanite, rutile and an unidentified Ca silicate. The new mineral is white and chalky in appearance, has a Mohs hardness of 5 and a measured density of 3.07(2) g/cm^3 (D_{calc} 3.13 g/cm^3), and shows little deviation from a uniaxial optical behavior (α 1.632, γ 1.649). Compositionally, it is an intermediate member of the ternary system $Ca_5(PO_4)_3(OH)$ – $Ca_5(PO_4)_3Cl$ – $Na_3Ca_2(SO_4)_3(OH)$. The average content of the latter two end-members is *ca.* 20 mol.% each. The combination of high Na and S contents (up to 0.63 and 0.71 apfu, respectively) is unparalleled by any previously reported natural composition, and indicates significant solubility of these elements in natural apatites even at low crystallization temperatures (< 400 °C). The monoclinic symmetry of this mineral, determined from microbeam X-ray diffraction patterns, distinguishes it from hydroxylapatite. By analogy with synthetic $Ca_5(PO_4)_3OH$, its space group is $P2_1/b$ [*a* 9.445(2) Å, *b* 18.853(4) Å, *c* 6.8783(6) Å, γ 120.00(2)°], and the deviation of symmetry from the archetypal (space group $P6_3/m$, *a* ~9.4 Å, *c* ~6.9 Å) probably results from ordering of $(OH)^-$ anions in [00*z*] anionic columns and consequent doubling of periodicity along [010]. In keeping with the nomenclature of apatites, this new mineral was named clinohydroxylapatite.

Key-words: clinohydroxylapatite, hydroxylapatite, Na-S-rich apatites, gabbro, Seagull pluton, Ontario.

Introduction

At present, the apatite group comprises some 30 mineral species, including members of the ternary series $Ca_5(PO_4)_3(F,OH,Cl)$, as well as structurally related phosphates, arsenates, silicates (and mixed Si-S and Si-B oxysalts), sulfates, and a vanadate. The number of species is approximate because some of them have not been formally approved by IMA, and are considered questionable (see Discussion). Members of the apatite group exhibit remarkable structural diversity arising from ordering of cations and/or anions relative to the archetypal structure (space group $P6_3/m$). Comprehensive reviews of the latter and its lower-symmetry derivatives have been written by Hughes & Rakovan (2002) and Rastsvetaeva & Khomyakov (1996). In the past 30 years, the continuously increasing interest toward apatite-type compounds in industry and science has prompted numerous detailed studies of the crystal chemistry of natural and synthetic compositions from the $Ca_5(PO_4)_3(F,OH,Cl)$ ternary series. This work has shown that synthetic $Ca_5(PO_4)_3(OH)$ and $Ca_5(PO_4)_3Cl$ crystallize with a monoclinic symmetry (space group $P2_1/b$), which changes reversibly to hexagonal upon heating (*e.g.*, Bauer & Klee, 1993; Takahashi *et al.*, 2001). The $P2_1/b$ polymorphs result from ordering of monovalent anions in [00*z*] columns. Prior to the present study, only naturally occurring chlorapatite had been shown to crystallize with both hexagonal and monoclinic symmetry (Hounslow & Chao, 1970; Hughes *et al.*, 1990), although no attempt was apparently made to have these different structural forms approved as distinct mineral species. Both hydroxylapatite (commonly referred to as "hydroxyapatite" in the materials-science literature) and fluorapatite had thus far been found in the geological setting only in hexagonal form. The described examples of hydroxylapatite, for which structural data are available, span a considerable range of compositions in terms of their OH, F, Cl and CO_2 contents (*e.g.*, Sudarsanan & Young, 1969; Sommerauer & Katz-Lehnert, 1985; Hughes *et al.*, 1991; Comodi *et al.*, 1999; Brigatti *et al.*, 2004). In this regard, note that the symmetry of the mineral hydroxylapatite is incorrectly given as $P2_1/b$ in the recent review by Pan & Fleet (2002, their Table 1).

DOI: 10.1127/0935-1221/2006/0018-0105
0935-1221/06/0018-0105 $ 3.60

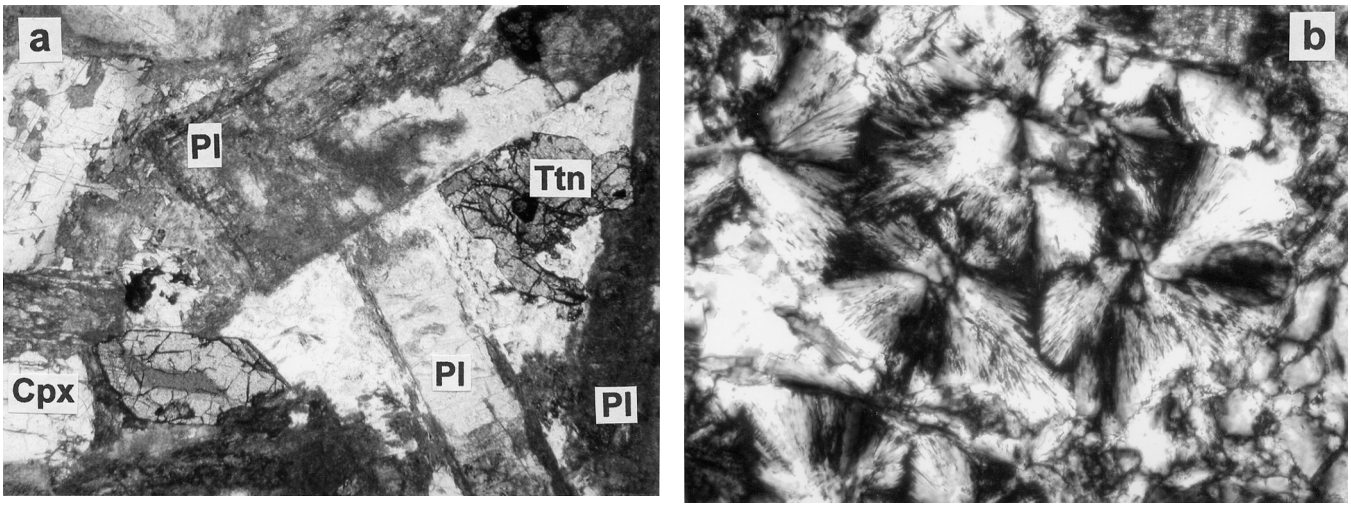

Fig. 1. The mode of occurrence of clinohydroxylapatite. (a) Ophitic-textured gabbro with large laths of altered plagioclase (P1), interstitial clinopyroxene (Cpx) an euhedral titanite (Ttn); plane-polarized light, field of view (FOV) 4.5 mm. (b) Spherulites of clinohydroxylapatite replacing plagioclase; crossed polars, FOW 50 μm.

A rock sample (~0.5 kg in weight), submitted to one of us (ARC) for petrographic analysis, was found to contain an apatite-group mineral with unusual chemical and optical characteristics (*i.e.*, high Na and S contents, and low refraction indices). A detailed examination of this material by a variety of methods showed it to be a monoclinic counterpart of hydroxylapatite. In keeping with the accepted nomenclature of apatite-group minerals, this new mineral was named clinohydroxylapatite. Both the mineral and its name were approved by the Commission on New Minerals and Mineral Names of the International Mineralogical Association (vote IMA 2004-006). The type material is deposited at the R.B. Ferguson Museum of Mineralogy, University of Manitoba (Canada).

Occurrence, paragenesis and properties

The samples containing clinohydroxylapatite were collected from a prospecting trench located between the Seagull and Leckie Lakes, *ca*. 7.5 km SSW of the Wolf Mountain and 50 km W of the town of Nipigon, Thunder Bay District, northwestern Ontario, Canada (Latt. 49º02' N; Long. 88º58' W). The UTM coordinates of the sampling location are 5432500m N and 356600m E (Zone 16) on NTS sheet 52 H/2. The host rock is a profusely altered leucogabbro probably representing one of the upper units in the Seagull intrusion of ultramafic and mafic rocks. The intrusion is a lopolith-like body of Mesoproterozoic age (*ca.* 1.11 Ga), emplaced along or near the contact between the metasedimentary rocks of the Sibley group (>1.45 Ga) and underlying Archean rocks. Further details on the regional geology and a schematic geological map of the Seagull Lake area can be found in Hart (2002) and Hart & Whaley (2004).

The host rock shows a recognizable (although somewhat obscured by subsolidus processes) ophitic texture, and is inferred to have originally comprised *ca.* 75 % of plagioclase, 25 % of clinopyroxene and subordinate ilmenite (Fig. 1a). The plagioclase of unknown composition was completely replaced by deuteric Ca phases, including prehnite, hibschite, a Ca silicate (tobermorite?) and clinohydroxylapatite, and subsequently by a montmorillonite-type clay. The primary clinopyroxene was preserved from alteration, whereas the ilmenite was partially replaced by titanite and rutile. Also present are hornblende (*sensu lato*) and very minor sphalerite, whose paragenetic relationships with clinohydroxylapatite are uncertain. Clinohydroxylapatite and the associated Ca silicates formed by late-stage hydrothermal alteration of the primary mineral assemblage (chiefly, plagioclase and ilmenite).

Clinohydroxylapatite occurs as masses of coalescent spherulites < 30 μm in diameter composed of acicular crystals; inclusions of other minerals were not observed. Individual crystals are elongate parallel to their [001] axes, and do not exceed a few μm in thickness (Fig. 1b). In hand specimen, the mineral is white, opaque and has a dull (chalky) luster; in plane-polarized light, it is colorless and transparent. Clinohydroxylapatite is brittle (with a splintery fracture in aggregates), devoid of cleavage or parting, and has a Mohs hardness of 5 (approximated by scratching the surface of a thin section with hardness picks). Its Vickers microhardness could not be determined owing to the small size of crystals. The density, measured in heavy liquids (di-iodomethane diluted with monobromonaphtalene), is 3.07(2) g/cm^3, which compares reasonably well with the calculated density of 3.13 g/cm^3.

Composition and formula

The composition of clinohydroxylapatite was determined by energy-dispersive X-ray spectrometry (EDS) using a Jeol 5900 LV scanning-electron microscope equipped with a LINK ISIS analytical system incorporating a Super ATW Light Element Detector. EDS was preferred to wavelength-dispersive spectrometry (WDS) because the latter method

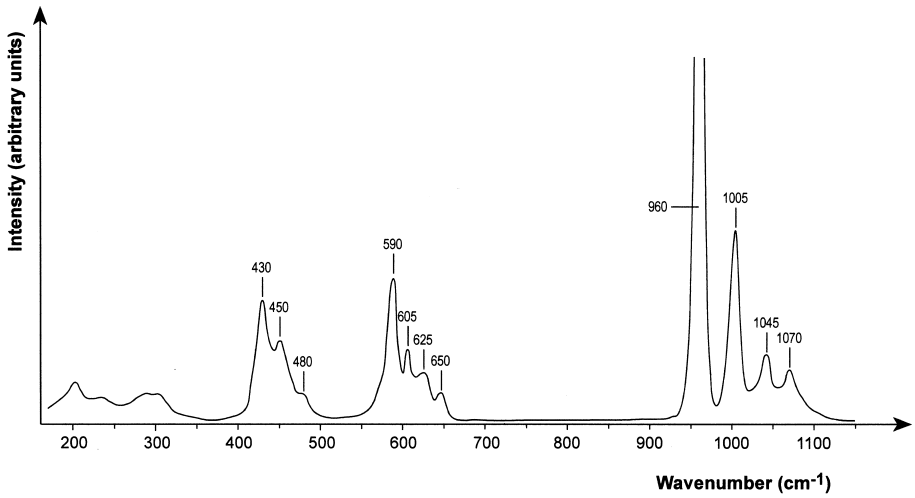

Fig. 2. Raman spectrum of clinohydroxylapatite.

Table 1. Clinohydroxylapatite: the average (1) and most Na-S-rich (2) compositions.

	1* wt.%	range	esd	2 wt.%		1* apfu	2 apfu
Na_2O	3.29	2.53- 3.88	0.34	3.88	Na	0.531	0.626
CaO	50.07	48.69-51.98	0.90	48.80	Ca	4.466	4.348
SrO	0.30	015- 0.48	0.09	0.29	Sr	0.015	0.014
La_2O_3	0.07	0- 0.47	0.12	0.30	La	0.002	0.009
Ce_2O_3	0.17	0- 0.50	0.17	0.24	Ce	0.005	0.007
SiO_2	0.19	0- 0.42	0.11	0.37	Si	0.016	0.031
P_2O_5	33.20	32.01-34.38	0.61	32.01	P	2.340	2.253
SO_3	10.01	8.21-11.40	0.91	11.40	S	0.625	0.712
Cl	1.64	1.19- 1.91	0.18	1.68	Cl	0.231	0.237
H_2O‡	1.38			1.38	OH	0.769	0.763
$-O=Cl_2$	0.37			0.38			
Total	99.95			99.97			

* Average of 28 electron-microprobe analyses.
‡ Wt.% H_2O calculated assuming stoichiometry.

employs higher beam currents and, hence, is more susceptible to the effects of Na loss and crystallographically controlled halogen diffusion (Stormer *et al.*, 1993). In our case, these effects would be difficult to mitigate due to the small size of spherulites and largely random orientation of crystals within the sample. Raw EDS spectra were acquired for 100 s (live time) with an accelerating voltage of 20 kV and a beam current of 0.65 nA. The spectra were processed using the LINK ISIS-SEMQUANT software, with full ZAF corrections applied. We used a 15×15 μm raster instead of a focused beam to avoid volatilization of Na, and monitored the acquisition of data to ensure that none of the analyzed elements exhibited a consistent loss or gain of counts. The following well-characterized standards were used for the analysis: Durango fluorapatite (Ca, P), jadeite (Na), chalcopyrite (S), wollastonite (Si), loparite-(Ce) (La, Ce), halite (Cl), and synthetic $SrTiO_3$ (Sr). F, Mn and Nd were sought, but not detected. The average of 28 electron-microprobe analyses and the most Na-S-rich composition are listed in Table 1.

The Raman spectrum of clinohydroxylapatite was measured using a Renishaw microspectrometer equipped with a 785-nm diode laser and automated *x-y* stage; crystalline Si was used as a calibration standard. The spectrum, obtained in quasiconfocal mode from an area *ca.* 3 μm across (Fig. 2), is characterized by the presence of $(PO_4)^{3-}$ and $(SO_4)^{2-}$ stretching and bending modes (ν_1 at 960 and 1005 cm^{-1}, respectively, and overlapping ν_4 between 590 and 650 cm^{-1}), $(OH)^-$ stretching modes at 3200–3250 cm^{-1}, and the absence of $(CO_3)^{2-}$ modes (Arkhipenko & Moroz, 1997; Comodi *et al.*, 1999). Hence, the available electron-microprobe and spectroscopic data indicate that S is the only significant substituent in the tetrahedrally coordinated sites, and that $(OH)^-$ and Cl^- are the only "tunnel" anions present in clinohydroxylapatite in detectable quantities. Accordingly, the amount of $(OH)^-$ was calculated from stoichiometry (*i.e.*, assuming O = 12 and Cl + OH = 1) and converted to wt.% H_2O. This calculation approach is validated by the fact that the cation totals in both cases are well within the standard analytical error from the stoichiometric values (Table 1). Imbalance between the total positive and negative charges is negligible (0.1 % of the smaller value), indicating that deviation of the clinohydroxylapatite composition from the ideal stoichiometry $[A_5(TO_4)_3X]$ is insignificant, if any. This conclusion is consistent with the lack of $(CO_3)^{2-}$ in the mineral inferred from the Raman spectrum.

The empirical formula of clinohydroxylapatite can be simplified to $(Ca,Na)_5[(P,S)O_4]_3(OH,Cl)$ or, disregarding the Na-S-Cl substitution, to $Ca_5[PO_4]_3(OH)$. The latter variant is preferable because Na-S-Cl-free clinohydroxylapatite should also be expected to exist in nature, especially taking into account that monoclinic $Ca_5[PO_4]_3(OH)$ can be readily synthesized using a variety of different methods (Table 2 and references therein), and that synthetic crystals containing a significant proportion of F or Cl also have a monoclinic symmetry (Rendón-Angeles *et al.*, 2000a, b).

X-ray diffraction

The recognition of clinohydroxylapatite as a new mineral species distinct from hydroxylapatite was based upon its examination by X-ray diffraction (XRD). We took particular care in data collection and ascertaining the monoclinic symmetry of this mineral. Due to the nature of the material, the

Table 2. Synthetic $Ca_5[PO_4]_3(OH)$: Preparation methods and unit-cell parameters.

Preparation method	*a*, Å	*b*, Å	*c*, Å	γ, °	D_{calc}	Other data	Reference
Hydroxylation of single-crystal $Ca_5(PO_4)_3Cl$ in H_2O steam at 1200 °C for 2 weeks	9.4214(8)	2 × *a*	6.8814(7)	120.00(8)	3.15	Structure by singlecrystal methods	Elliott *et al.*, 1973
Hydroxylation of single-crystal $Ca_5(PO_4)_3F$ in KOH solution at 800 °C and 1 kbar	Monoclinic, parameters not reported					IR spectra	Rendón-Angeles *et al.*, 2000a
Addition of HPO solution to CH suspension with subsequent aging for 3 days at room *T*, freeze-drying and heating at 1200 °C for 1 h	9.426(3)	18.856(5)	6.887(1)	119.97(1)	3.15	Structure by Rietveld method, IR spectrum	Ikoma *et al.*, 1999
Solid-state synthesis (1100 °C in vacuum, 900 °C in steam) from CO_2-bearing intermediate obtained by reaction of CC with CHP in solution at 80 °C	9.4225(15)	18.8465(28)	6.8845(1)	119.971(4)	3.15	Structure by Rietveld, FTIR spectra	Morgan *et al.*, 2000
Solid-state synthesis from CHPH and CC calcined and reacted in Ar+H_2O at 900 °C	9.4202(3)	18.8399(4)	6.8818(3)	120.001(1)	3.15	IR spectrum, differential scanning calorimetry (to 220 °C)	Takahashi *et al.*, 2001
High-*P* (1 kbar) synthesis from melt of CH and CP heated to 1450 °C and slowly cooled to 1100 °C	9.419(3)	18.848(6)	6.884(2)	119.98(2)	3.15	Structure by single crystal methods	Suetsugu & Tanaka, 2002
High-*P* (1.5 kbar, 650 °C) hydrothermal synthesis from a mixture of CaO, NHP and H_2O for 1–2 weeks	9.419(2)		6.879(1)		3.16	^{31}P and ^{1}H NMR spectra, FTIR spectra	Imbach *et al.*, 2002

HPO = H_3PO_4; CH = $Ca(OH)_2$; CC = $CaCO_3$; CHP = $CaHPO_4$; CHPH = $CaHPO_4{\cdot}2H_2O$; CP = $Ca_3(PO_4)_2$; NHP = $NH_4H_2PO_4$.

XRD pattern was measured *in situ*, from the same cluster of spherulites that was analyzed chemically. The XRD data were collected using CuKα radiation with a Rigaku D-max Rapid micro-diffractometer equipped with an image plate detector, a flat graphite monochromator, and a microscope for accurate sample positioning. To optimize the data-collection protocol, several trial experiments were carried out first under different operating conditions. These experiments differed in sample position (ϕ fixed, with an ω rotation range of 0–10°), X-ray beam power (1.20–1.36 kW), collimator diameter (50 and 100 μm), and data-collection time (0.5–24 h). The best results were obtained with the sample position fixed, at 40 kV and 34 mA, a beam diameter of 100 μm, and a data-collection time of 18 h. These data were further verified by additional data collections from the same area within the sample using a beam diameter of 50 μm and increasing collection times, but no significant improvement in reflection intensities was observed. The nature of the examined sample did not allow any peaks at $2\theta < 18°$ to be resolved.

The XRD data were collected as two-dimensional images and converted into 2θ-*I* profiles. After preliminary analysis of these profiles, four datasets obtained at different sample positions, but under identical operating conditions, were summed to minimize any differences in reflection intensities due to preferred orientation. The conversion and summation of the data were carried out using the Rigaku R-Axis Display software. The summary profile was carefully examined for any reflections that would indicate deviation from the archetypal $P6_3/m$ symmetry (see Introduction). This analysis enabled the detection of weak, but distinct reflections indicative of monoclinic symmetry and a doubled periodicity along the [010] axis (Table 3). These diffraction lines (*hkl*, where *k* = odd) are characteristically absent from XRD patterns of either hexagonal apatites (*e.g.*, hydroxylapatite, space group $P6_3/m$: Hughes *et al.*, 1989, 1991), or monoclinic apatites with an ordered distribution of small cations in the tetrahedrally-coordinated sites (*e.g.*, hydroxylellestadite, space group $P2_1/m$: Hughes & Drexler, 1991). To our knowledge, this type of reflections is observed only in apatite-type compounds whose symmetry is lowered to monoclinic (space group $P2_1/b$) owing to ordering of the monovalent anions in adjacent structural tunnels (*e.g.*, Elliott *et al.*, 1973). The doubling of periodicity along [010] results from conversion of the mirror plane to a *b* glide plane perpendicular to [001]. Such symmetry-breaking has been previously reported for natural and synthetic chlorapatite, and synthetic $Ca_5(PO_4)_3(OH)$ (*ibid.*; Elliott *et al.*, 1973;

Table 3. X-ray powder diffraction data for clinohydroxylapatite.

I	$d_{meas.}$	$d_{calc.}$	*h k l*
1	4.261	4.268	0 3 1
1	4.085	4.086	-2 4 0
5	3.895	3.893	-2 2 1
1	3.789	3.788	-2 1 1
20	**3.440**	**3.439**	**0 0 2**
1	3.361	3.365	0 1 2
1	3.236	3.232	-1 1 2
5	3.171	3.169	0 2 2
9	3.084	3.090	2 2 0
1	3.009	3.005	1 1 2
1	2.949	2.950	0 5 1
1	2.902	2.907	0 3 2
66	**2.817**	**2.815**	**-1 6 1**
41	**2.781**	**2.778**	**-1 4 2**
79	**2.724**	**2.721**	**0 6 0**
24	**2.630**	**2.631**	**-2 4 2**
5	2.529	2.530	0 6 1
18	2.499	2.501	-2 7 1
1	2.475	2.476	2 1 2
1	2.443	2.445	1 5 1
3	2.370	2.368	0 5 2
13	2.297	2.296	-1 6 2
100	**2.267**	**2.268**	**3 2 0**
2	2.233	2.231	2 4 1
3	2.206	2.207	0 2 3
8	2.150	2.150	-1 8 1
9	2.136	2.137	3 0 2
9	2.062	2.062	1 2 3
5	2.042	2.041	0 8 0
5	1.999	2.000	2 0 3
39	**1.945**	**1.945**	**2 4 2**
15	1.892	1.892	1 6 2
3	1.875	1.877	-5 4 0
58	**1.841**	**1.841**	**2 2 3**
21	**1.807**	**1.807**	**-3 10 1**
70	**1.784**	**1.784**	**4 2 0**
14	1.755	1.755	0 8 2
9	1.719	1.720	0 0 4
2	1.681	1.683	0 2 4
6	1.645	1.646	2 6 2
8	1.613	1.613	-4 2 3
2	1.588	1.589	0.10.1
9	1.543	1.544	2 8 0
9	1.503	1.503	2 2 4
10	1.477	1.477	5 0 2
19	1.454	1.454	0 6 4
10	1.435	1.434	1.10.1
3	1.349	1.349	1.10.2
6	1.283	1.282	-6 4 3
8	1.256	1.257	2 2 5
13	1.236	1.236	-6.10.3
7	1.222	1.222	2.10.2
5	1.160	1.160	3 6 4
4	1.114	1.114	1 2 6
6	1.106	1.106	5 6 2
7	1.031	1.031	2 4 6
4	1.009	1.009	0.16.1
3	1.004	1.004	1.15.1
4	0.973	0.973	1.15.2
4	0.950	0.951	1 3 7
1	0.938	0.938	0.10.6
2	0.937	0.936	2 2 7
3	0.877	0.877	0.18.2

Ten strongest lines are given in bold.

Hughes *et al.*, 1990; Ikoma *et al.*, 1999). Note also that ordering of Ca and Na over the positions with a nine- and seven-fold coordination will not produce the same structural effect. Both natural $Na_3Ca_2(SO_4)_3(OH)$ (cesanite) and synthetic $Na_{3.2\text{-}3.3}Ca_{1.8\text{-}1.7}(SO_4)_3(F,Cl)_{0.7\text{-}0.8}$ are hexagonal apatites crystallizing with the $P6_3/m$ symmetry (Deganello, 1983; Piotrowski *et al.*, 2002). Synthetic "carbonate-hydroxylapatite" with 0.4 apfu Na is also hexagonal (El Feki *et al.*, 2000). Hence, we infer that $P2_1/b$ is the correct space group for clinohydroxylapatite, and that the observed monoclinic distortion probably arises from ordering of the anions in the structural tunnels, and not from ordering of cations in either tetrahedrally coordinated or larger Ca sites.

The XRD pattern of clinohydroxylapatite was indexed on a $P2_1/b$ cell, and its unit-cell parameters refined from a total of 64 reflections (Table 3) using the UnitCell software (Holland & Redfern, 1997). It is noteworthy here that the cluster of spherulites examined by XRD is devoid of inclusions and is sufficiently large to avoid excitation of the surrounding material. Although weak, the observed superlattice peaks indicative of monoclinic symmetry are comparable in intensity to those in the XRD pattern of synthetic $Ca_5(PO_4)_3(OH)$ (Ikoma *et al.,* 1999, p. 274). Thus, we are confident that all diffraction lines listed in Table 3 correspond to clinohydroxylapatite. Accurate refinement of the crystal structure of clinohydroxylapatite by the Rietveld method is hindered by the paucity of material. Because our interpretation that the monoclinic symmetry of clinohydroxylapatite results from ordering of the monovalent anions could not be confirmed experimentally, we shall not provide any details on the hypothetical monoclinic structural model here. Various aspects of anion ordering in synthetic apatites and natural chlorapatite have been covered extensively in the literature (*e.g.*, Elliott *et al.*, 1973; Hughes *et al.*, 1990; de Leeuw, 2002).

Discussion

Crystal chemistry

Element-variation diagrams (Fig. 3) show a positive correlation between Na and S, and inverse correlations between Na and Ca, as well as S and P. The amount of Cl ranges from 0.17–0.27 atoms per formula unit (apfu), but does not show any systematic variation with Na or S content. Hence, in terms of composition, the Seagull material is intermediate between $Ca_5(PO_4)_3(OH)$, $Ca_5(PO_4)_3Cl$ and $Na_3Ca_2(SO_4)_3(OH)$ (*ca.* 60, 20 and 20 mol. %, respectively, for the average composition). Sodian-sulfatian varieties of apatite appear to be rare in nature. The extent of $Na^{1+}S^{6+}(Ca^{2+}P^{5+})_{-1}$ substitution observed in the present study (Table 1) is unparalleled by any naturally occurring apatite described in the previously published literature. The most Na-S-rich composition reported to date is fluorapatite from the Kushikino mine in Japan, containing up to 0.36 apfu Na and 0.41 S (Shiga & Urashima, 1987). Cesanite $Na_3Ca_2(SO_4)_3(OH)$ is not known outside its type locality at Cesano, Italy. The data available in the literature (Harada *et al.*, 1971; Rouse & Dunn, 1982; Hogarth, 1988; Litsarev *et al.*, 1998; Grabezhev *et al.*, 2004)

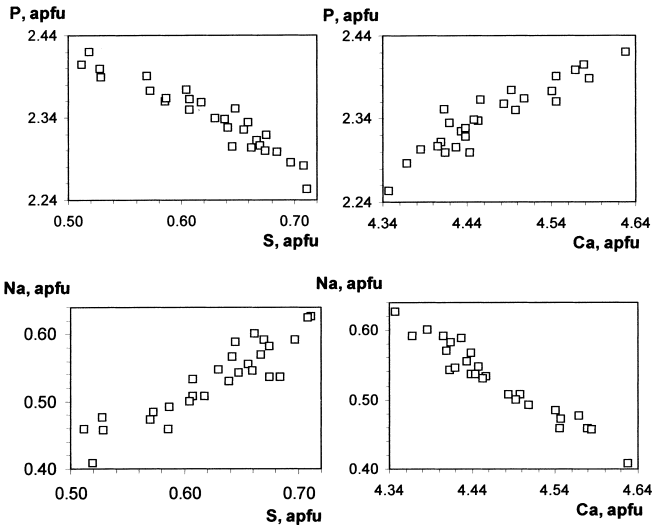

Fig. 3. Interelement correlations in clinohydroxylapatite (apfu values given relative to a total of 8 cations per formula unit).

indicate that the alternative substitution $Si^{4+}S^{6+}(P^{5+})_{-2}$ is of greater significance to S-rich apatite-group minerals of metasomatic or hydrothermal origin. Igneous apatites (*sensu lato*) generally contain lower levels of S (≤ 3.9 wt.% SO_3: Comodi *et al.*, 1999), and it is unclear at present which of the discussed substitution mechanisms is the preferred mode of S incorporation in these apatites (*cf.* Peng *et al.*, 1997 and Comodi *et al.*, 1999).

Crystallization conditions

Clinohydroxylapatite is a metasomatic phase produced by reaction of primary plagioclase with sulfate-bearing fluids. Assuming that clinohydroxylapatite is syngenetic with prehnite, the upper temperature limit of metasomatism could be set at 380 °C (Strens, 1968; Gurevich & Ivanov, 1977). For comparison, the sodian-sulfatian fluorapatite from Kushikino is believed to have crystallized at 200–250 °C (Shiga & Urashima, 1987). The enrichment of the Seagull clinohydroxylapatite in $(SO_4)^{2-}$ and the paucity of sulfide minerals in its host rock indicate a high oxygen fugacity in the fluid. At present, the source of this fluid is uncertain. It could have been derived from, or modified through interaction with, the sulfate-enriched metasedimentary rocks of the Sibley group. The petrographic evidence of such interaction includes the occurrence of calc-silicate metasomatic assemblages along the contact between the Sibley group and intrusion, and of K-rich monzogabbro units within the intrusion (Hart & Whaley, 2004).

Hexagonal or monoclinic?

In synthetic systems, the transition of monoclinic $Ca_5(PO_4)_3(OH)$ to a hexagonal (anion-disordered) form occurs at *ca.* 205 °C (Takahashi *et al.*, 2001). It is likely shifted to higher temperatures for Cl-bearing compositions, because the transition temperature in $Ca_5(PO_4)_3Cl$ is about 350 °C (Bauer & Klee, 1993). Unfortunately, however, these data cannot be applied directly to the assessment of crystallization temperature of natural samples. Firstly, synthetic crystals grown at high temperatures (Table 2) readily assume the monoclinic structure upon cooling, which is clearly not the case for natural hydroxylapatite, even including its near-stoichiometric examples (*e.g.*, Hughes *et al.*, 1989). This discrepancy may indicate potential importance of unknown kinetic parameter(s). Alternatively, Elliott *et al.* (1973) have suggested that the orientation of $(OH)^-$ in the structure of natural hydroxylapatite is locally ordered, but F impurities, ubiquitous in this mineral, act as "reversal points" for $(OH)^-$, giving rise to the overall hexagonal symmetry. This view was supported by Hughes *et al.* (1989), who suggested that "if insufficient F anions or vacancies (< 0.15 per site?) exist in the anion columns, OH anions will order above the plane in a given column and below the plane in the adjacent column along *b*, giving rise to monoclinic $P2_1/b$ symmetry" (p. 874). Electronic-structure calculations (de Leeuw, 2002) have shown that replacement of *ca.* 30% of $(OH)^-$ by F^- is energetically favorable and randomizes the orientation of hydroxyl groups in the anionic columns. However, this model is difficult to reconcile with the fact that synthetic crystals of composition $Ca_5(PO_4)_3(OH_{0.6\text{-}0.8}F_{0.2\text{-}0.4})$ are monoclinic (Rendón-Angeles *et al.*, 2000a). It is possible that the material synthesized in the latter study comprises both hexagonal (relatively F-rich) and monoclinic (F-poor) submicroscopic domains, but this suggestion is purely speculative. Hence, the effect of substituent atoms (especially F and Cl) on the hexagonal-to-monoclinic transition in apatites is by and large uncertain.

Finally, density functional theory calculations show that the monoclinic form of $Ca_5(PO_4)_3(OH)$ has virtually no energetic advantage over the disordered hexagonal form (de Leeuw, 2002; Calderín *et al.*, 2003). It is thus to be expected that hydoxylapatite may also form metastably at temperatures below the transition. All these uncertainties combined render any attempt to predict the symmetry of a random OH-dominant apatite composition futile. Our work demonstrates that distinguishing between the hexagonal and monoclinic variants is not a trivial matter even when assisted by modern instrumental techniques. Hence, some of the material described in the published literature as hydroxylapatite may, in fact, be clinohydroxylapatite.

Relationship to other minerals and implications for the apatite-group nomenclature

Clinohydroxylapatite is a member of the apatite mineral group dimorphous with hexagonal hydroxylapatite. Relative to pure $Ca_5(PO_4)_3(OH)$, the Seagull material contains a high proportion of S, Na and Cl, which is reflected in its properties (Table 4). Samples of clinohydroxylapatite devoid of these impurities should be expected to have refraction indices and density similar to those of hydroxylapatite, given the relatively subtle structural difference between these two minerals.

It is noteworthy here that the amount of $(SO_4)^{2-}$ in the examined clinohydroxylapatite far exceeds the proportion of

Table 4. Clinohydroxylapatite and related apatite-group minerals: Comparison of physical and structural characteristics.

Name	Clinohydroxylapatite	Hydroxylapatite	Cesanite
Simplified formula	$Ca_5(PO_4)_3(OH)$	$Ca_5(PO_4)_3(OH)$	$Na_3Ca_2(SO_4)_3(OH)$
Symmetry system	Monoclinic	Hexagonal	Hexagonal
Space group	$P2_1/b$	$P6_3/m$	$P6_3/m$
Unit-cell parameters*:			
a, Å	9.445(2)	9.4166	9.446(1)
b, Å	18.853(4)	9.4166	9.446(1)
c, Å	6.8783(6)	6.8745	6.895(1)
γ, °	120.00 (2)	120.00	120.00
Z	4	2	2
Density, g/cm^3:			
measured	3.07	3.21	2.79
calculated*	3.13	3.16	2.71
Refractive indices:			
ω(or γ)	1.640	1.651‡	1.570
ε(or α)	1.632	1.644‡	1.564
References:	this work	Hughes *et al.* (1989)	Deganello (1983)
		Mitchell (1943)	Cavaretta *et al.* (1981)

* See Table 2 for unit-cell parameters and calculated densities of synthetic $Ca_5(PO_4)_3(OH)$.
‡ Indices for synthetic material are 1.6504 and 1.6449 (Jullmann & Mosebach, 1966).

$(CO_3)^{2-}$ anions in any of "carbonate-apatites" described in the literature to date. The highest carbon content reported for apatite is 4.4 wt. % CO_2 or *ca.* 0.45 apfu C (modern-bone apatite of Brophy & Nash, 1968), whereas the maximum sulfur content in the clinohydroxylapatite is 0.71 apfu S (11.4 wt. % SO_3), and the average content is 0.62 apfu S. In some literature, carbonate-rich members of the apatite group are referred to as "carbonate-hydroxylapatite" and "carbonate-fluorapatite" (*e.g.*, Mandarino & Back, 2004). Consequently, we included in our proposal the name "sulfate-hydroxylapatite" as a possible alternative to clinohydroxylapatite, and requested that the members of CNMMN comment, *pro vel contra*, on these two alternative names. Of the 14 Commission members that responded to our request, the overwhelming majority (11) favored clinohydroxylapatite, emphasizing that the name "sulfate-hydroxylapatite" would only be appropriate if S^{6+} were the predominant cation in the tetrahedral sites (*i.e.* for compositions with > 1.5 apfu S), and that neither "carbonate-hydroxylapatite" nor "carbonate-fluorapatite" have been formally approved by CNMMN. These comments put the validity of these names in question, especially taking into account that they have been applied in the literature to compositions with as little as 0.2 wt. % CO_2 (*e.g.*, Chang *et al.*, 1996, p. 310).

Another interesting implication of the present work is that monoclinic $Ca_5(PO_4)Cl$ studied by Hounslow & Chao (1970) also deserves the recognition as a mineral species distinct from hexagonal chlorapatite (*e.g.*, samples from Kragerø, Norway: Hughes *et al.*, 1989). Clearly, the existing nomenclature of the apatite mineral group is in need of critical revision.

Acknowledgements: This work was supported in part by the University of Manitoba Research Grants Program, and by the Natural Sciences and Engineering Research Council of Canada (ARC). The valuable advice of Ermanno Galli (University of Modena) on X-ray data collection is cordially acknowledged. We are also grateful to Donald Bubar (President, Avalon Ventures Ltd.) for his kind permission to use the samples collected as part of his company's exploration program, and for having provided us with detailed information on the provenance of these samples. Kelly Akers and Allan MacKenzie are thanked for their help with the acquisition of Raman spectra and electron-microprobe data, respectively. We are grateful to John Hughes, Sabrina Nazzareni and Tom Hart for their constructive comments on the earlier version of this paper. The comments made by Ernst Burke (Chairman) and other members of CNMMN on our proposal and the apatite-group nomenclature are also much appreciated.

References

Arkhipenko, D.K. & Moroz, T.N. (1997): Vibrational spectrum of natural ellestadite. *Kristallogr.*, **42**, 711-716.

Bauer, M. & Klee, W.E. (1993): The monoclinic-hexagonal phase transition in chlorapatite. *Eur. J. Mineral.*, **5**, 307-316.

Brigatti, M.F., Malferrari, D., Medici, L., Ottolini, L., Poppi, L. (2004): Crystal chemistry of apatites from the Tapira carbonatite complex, Brazil. *Eur. J. Mineral.*, **16**, 677-685.

Brophy, G.P. & Nash, J.T. (1968): Compositional, infrared, and X-ray analysis of fossil bone. *Am. Mineral.*, **53**, 445-454.

Calderín, L., Stott, M.J., Rubio, A. (2003): Electronic and crystallographic structure of apatites. *Phys. Rev. B*, **67**, 134106 – 1-7.

Cavaretta, G., Mottana, A., Tecce, F. (1981): Cesanite, $Ca_2Na_3[(OH)(SO_4)_3]$, a sulphate isotypic to apatite, from the Cesano geothermal field. *Mineral. Mag.*, **44**, 269-273.

Chang, L.L.Y., Howie, R.A., Zussman, J. (1996): Rock-Forming Minerals. Volume 5B. Non-silicates: Sulphates, Carbonates, Phosphates, Halides, 383 p. Longman Group Ltd, Burnt Mill.

Comodi, P., Liu, Y., Stoppa, F., Woolley, A.R. (1999): A multi-method analysis of Si-, S- and *REE*-rich apatite from a new find of kalsilite-bearing leucitite (Abruzzi, Italy). *Mineral. Mag.*, **63**, 661-672.

Deganello, S. (1983): The crystal structure of cesanite at 21 and 236 °C. *Neues Jahrb. Mineral. Monatsh.*, **1983** (7), 305-313.

El Feki, H., Savariault, J.M., Ben Salah, A., Jemal, M. (2000): Sodium and carbonate distribution in substituted calcium hydroxyapatite. *Solid State Sci.*, **2**, 577-586.

Elliott, J.C., Mackie, P.E., Young, R.A. (1973): Monoclinic hydroxyapatite. *Science*, **180**, 1055-1057.

Grabezhev, A.I., Gmyra, V.G., Pal'gueva, G.V. (2004): Hydroxylellestadite metasomatites from the Gumeshev skarn porphyry copper ore deposit, Central Urals. *Doklady Earth Sci.*, **395**, 196-198.

Gurevich, L. P. & Ivanov, I. P. (1977): Stability of prehnite in metabasites according to experimental data. *Ocherki Fiz.-Khim. Petrol.*, **6**, 54-60 (in Russ.).

Harada, K., Nagashima, K., Kato, A. (1971): Hydroxylellestadite, a new apatite from Chichibu Mine, Saitama Prefecture, Japan. *Am. Mineral.*, **56**, 1507-1518.

Hart, T.R. (2002): Project Unit 02-005. Reconnaissance survey of the Proterozoic mafic and ultramafic intrusions of the southern portion of the Nipigon embayment. *Ontario Geol. Surv. Open File Rep.*, **6100**, 12: 1-10.

Hart, T.R., Whaley, A.G. (2004): Project Unit 03-001. Lake Nipigon region geoscience initiative. Proterozoic and Archean geology of the southern area of the western Nipigon Embayment. *Ontario Geol. Surv. Open File Rep.*, **6145**, 48: 1-11.

Hogarth, D.D. (1988): Chemical composition of fluorapatite and associated minerals from skarn near Gatineau, Quebec. *Mineral. Mag.*, **52**, 347-358.

Holland, T.J.B. & Redfern, S.A.T. (1997): Unit cell refinement from powder diffraction data: the use of regression diagnostics. *Mineral. Mag.*, **61**, 65-77.

Hounslow, A.W. & Chao, G.Y. (1970): Monoclinic chlorapatite from Ontario. *Can. Mineral.*, **10**, 252-259.

Hughes, J.M. & Drexler, J.W. (1991): Cation distribution in the apatite tetrahedral site: Crystal structures of type hydroxylellestadite and type fermorite. *Neues Jahrb. Mineral. Monatsh.*, **1991** (7), 327-336.

Hughes, J.M. & Rakovan, J. (2002): The crystal structure of apatite, $Ca_5(PO_4)_3(F,OH,Cl)$. In: P.H. Ribbe & J.J. Rosso, Eds., Phosphates: Geochemical, Geobiological, and Materials Importance. Reviews in Mineralogy & Geochemistry, Vol. **48**, p. 1-12. Mineral. *Soc. America*, Washington (DC).

Hughes, J.M., Cameron, M., Crowley, K.D. (1989): Structural variations in natural F, OH and Cl apatites. *Am. Mineral.*, **74**, 870-876.

–, –, – (1990): Crystal structures of natural ternary apatites: Solid solution in the $Ca_5(PO_4)_3X$ (X = F, OH, Cl) system. *Am. Mineral.*, **75**, 295-304.

Hughes, J.M., Cameron, M., Mariano, A.N. (1991): Rare-earth-element ordering and structural variations in natural rare-earth-bearing apatites. *Am. Mineral.*, **76**, 1165-1173.

Ikoma, T., Yamazaki, A., Nakamura, S., Akao, M. (1999): Preparation and structure refinement of monoclinic hydroxylapatite. *J. Solid State Chem.*, **144**, 272-276.

Imbach, J., Brunet, F., Charpentier, T., Virlet, J. (2002): Synthesis and NMR characterization (^1H and ^{31}P MAS) of the fluorine-free hydroxylapatite-britholite-(Y) series. *Am. Mineral.*, **87**, 947-957.

Jullmann, H. & Mosebach, R. (1966): The synthesis, refractivity, and birefringence of hydroxylapatite. *Zeit. Naturf. B*, **21**, 493-494.

de Leeuw, N.H. (2002): Density functional theory calculations of local ordering of hydroxyl groups and fluoride ions in hydroxylapatite. *Phys. Chem. Chem. Phys.*, **4**, 3865-3871.

Litsarev, M.A., Organova, N.I., Khranach, P., Chukanov, N.V., Kuz'mina, O.V., Kartashov, P.M., Laputina, I.P., Zadov, A.E. (1998): Hydroxylellestadite from the garnet-wollastonite skarns of Arimao-Norte (Cuba). *Zapiski Vseross. Mineral. Obshch.*, **127** (6), 68-75.

Mandarino, J.A. & Back, M.E. (2004): Fleischer's Glossary of Mineral Species 2004. 309 p. Mineral. Rec. Inc., Tucson (Arizona).

Mitchell, L., Faust, G.T., Hendricks, S.B., Reynolds, D.S. (1943): The mineralogy and genesis of hydroxyapatite. *Am. Mineral.*, **28**, 356-371.

Morgan, H., Wilson, R.M., Elliot, J.C., Dowker, S.E.P., Anderson, P. (2000): Preparation and characterisation of monoclinic hydroxyapatite and its precipitated carbonate apatite intermediate. *Biomater.*, **21**, 617-627.

Pan, Yu. & Fleet, M.E. (2002): Compositions of the apatite-group minerals: substitution mechanisms and controlling factors. In: P.H. Ribbe & J.J. Rosso, Eds., Phosphates: Geochemical, Geobiological, and Materials Importance. Reviews in Mineralogy & Geochemistry, Vol. **48**, p. 13-49. Mineral. Soc. America, Washington (DC).

Peng, G., Luhr, J.F., McGee, J.J. (1997): Factors controlling sulfur concentrations in volcanic apatite. *Am. Mineral.*, **82**, 1210-1224.

Piotrowski, A., Kahlenberg, V., Fischer, R.X. (2002): The solid solution series of the sulfate apatite system $Na_{6.45}Ca_{3.55}(SO_4)_6(F_xCl_{1-x})_{1.55}$. *J. Solid State Chem.*, **163**, 398-405.

Rastsvetaeva, R.K. & Khomyakov, A.P. (1996): Structural features of a new naturally occurring representative of the fluorapatite-deloneite series. *Crystallogr. Rep.*, **41**, 789-792.

Rendón-Angeles, J.C., Yanagisawa, K., Ishizawa, N., Oishi, S. (2000a): Conversion of calcium fluorapatite into calcium hydroxyapatite under alkaline hydrothermal conditions. *J. Solid State Chem.*, **151**, 65-72.

–, –, –, – (2000b): Effect of metal ions of chlorapatites on the topotaxial replacement by hydroxyapatite under hydrothermal conditions. *J. Solid State Chem.*, **154**, 569-578.

Rouse, R.C. & Dunn, P.J. (1982): Contribution to the crystal chemistry of ellestadite and the silicate sulfate apatites. *Am. Mineral.*, **67**, 90-96.

Shiga, Yo. & Urashima, Yu. (1987): A sodian sulfatian fluorapatite from an epithermal calcite-quartz vein of the Kushikono mine, Kagoshima Prefecture, Japan. *Can. Mineral.*, **25**, 673-681.

Sommerauer, J. & Katz-Lehnert, K. (1985): A new partial substitution mechanism of CO_3^{2-}/CO_3OH^{3-} and SiO_4^{4-} for the PO_4^{3-} group in hydroxylapatite from the Kaiserstuhl alkaline complex (SW-Germany). *Contrib. Mineral. Petrol.*, **91**, 360-368.

Stormer, J.C., Pierson, M.L., Tacker, R.C. (1993): Variation of F and Cl X-ray intensity due to anisotropic diffusion in apatite during electron microprobe analysis. *Am. Mineral.*, **78**, 641-648.

Strens, R.G.J. (1968): Reconnaissance of the prehnite stability field. *Mineral. Mag.*, **36**, 864-867.

Sudarsanan, K. & Young, R.A. (1969): Significant precision in crystal structural details: Holly Springs hydroxylapatite. *Acta Cryst. B*, **25**, 1534-1543.

Suetsugu, Y. & Tanaka, J. (2002): Crystal growth and structure analysis of twin-free monoclinic hydroxylapatite. *J. Mater. Sci.*, **13**, 767-772.

Takahashi, H., Yashima, M., Kakihana, M., Yoshimura, M. (2001): A differential scanning calorimeter study of the monoclinic (P21/b) ↔ hexagonal (P63/m) reversible phase transition in hydroxylapatite. *Termochim. Acta*, **371**, 53-56.

Received 16 February 2005
Modified version received 20 June 2005
Accepted 19 September 2005